Supporting Information for "Gauging van der Waals Interactions in Aqueous Solutions of 2D MOFs: When Water Likes Organic Linkers More than Open-metal Sites"

Mohammad R. Momeni*, Zeyu Zhang, David Dell'Angelo, and Farnaz A. Shakib*

Department of Chemistry and Environmental Science, New Jersey Institute of Technology, Newark 07102, NJ United States

E-mail: momeni@njit.edu,shakib@njit.edu

Contents

References **27**

S1. Developing *ab initio* force fields and periodic electronic structure calculations

Starting from the experimental crystallographic data available for $Co_3(HHTP)_2$,[1] we built a 2×2×2 super cell for the dry MOF by removing hydrolyzed layers, and all chemisorbed water molecules and adjusting the interlayer distances to ∼4 Å. Both cell vectors and atomic positions of this supercell was minimized with periodic boundary conditions using the PBE[2] density functional with damped D3 dispersion correction[3] in CP2K version 5.1.[4] The molecularly optimized DZVP-MOLOPT basis sets and core-electron pseudopotentials according to the Geodecker-Teter-Hutter formulation[5] were used. For all studied MOFs, spin-polarized calculations were performed. The plane-wave cutoff of the finest grid and REL_CUTOFF were set to 400 and 60 Ry, respectively. The default value of 10^{-5} Ry was used for all SCF convergences.

Force field parameters for transition metals do not exist in Generic force fields such as generalized amber force field (GAFF).[6] Here, David Carrol's genetic algorithm[7] was used for fitting all interactions involving the Cu^{2+} transition metal centers including bonds, angles, and dihedrals while all parameters involving the intramolecular interactions present in the organic linkers were taken from GAFF without further modification. For creating the training sets, reduced cluster models comprised of a single Cu center and two truncated linkers were cut from the optimized crystal structures, Figure S1. The central metal atoms were then displaced by 0.02 Å from -0.04 Å to +0.04 Å along the x, y and z dimensions (creating a total of 125 configurations). All electronic energies for this training set were then calculated using the ωB97M-v[8] density functional and the def2-TZVP basis set as implemented in QCHEM 5.2.[9] To fit force field parameters to this *ab initio* training set, Morse potential was used for all coordinative metal-oxo bonds while Harmonic potential was employed for the rest. Atomic charges were computed at the ωB97X-d/def2-TZVP level[8] using the CHELPG scheme which fits all atomic charges to represent molecular electrostatic potential.[10] The
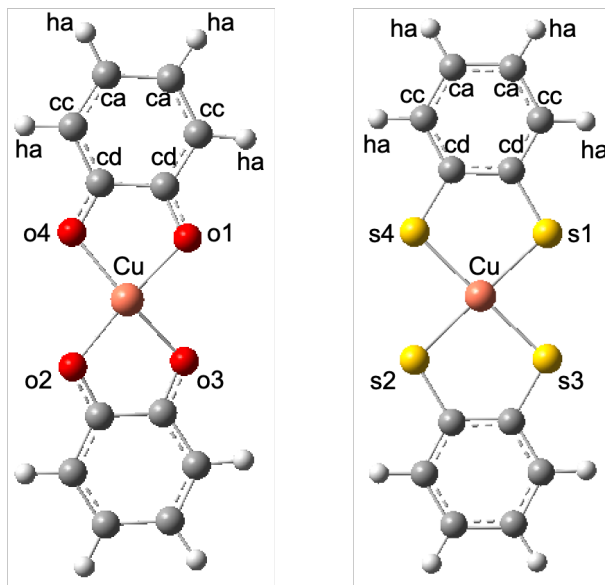
Figure S1: Cluster models with the atom labels used in developing *ab initio* force fields for $Cu_3(HHTP)_2$ and $Cu_3(HTTP)_2$ 2D MOFs.

unrestricted formalism was used for all calculations with charge of zero and spin multiplicity of 2. The complete list of the bonded and non-bonded parameters for $Cu_3(HHTP)_2$ and $Cu_3(HTTP)_2$ MOFs are given in Tables S1-S5 and S6-S10, respectively. The Lennard-Jones parameters for Cu were taken from the Universal Force Field (UFF).[11]

Table S1: Electrostatic and Lennard-Jones non-bonded parameters for $Cu_3(HHTP)_2$ MOF where r_{ij} refers to the distance between two atoms.

$$V_{LJ}(r) = 4\epsilon\left[\left(\frac{\sigma}{r_{ij}}\right)^{12} - \left(\frac{\sigma}{r_{ij}}\right)^{6}\right] \tag{1}$$

Atom name	Atom type	Charge	ε (kcal·mol^{-1})	σ / 2 (Å)
Cu	Cu	1.2399	0.00500	1.55700
o1	o1	-0.6004	0.17000	1.50001
o2	o2	-0.6794	0.17000	1.50001
o3	o3	-0.6495	0.17000	1.50001
o4	o4	-0.6242	0.17000	1.50001
cd	C	0.3795	0.08600	1.69983
cc	C	-0.1251	0.08600	1.69983
ca	C	-0.0889	0.08600	1.69983
ha	H	0.1629	0.01500	1.29982

Table S2: Harmonic bond potential parameters for $Cu_3(HHTP)_2$ MOF.

$$V_{bond}(r) = \frac{1}{2}K_{ij}(r_{ij} - r_0)^2 \qquad (2)$$

Bond type (Harmonic)	K_{ij}(kcal mol^{-1}Å^{-2})	r_0(Å)
cd-o1	1039.400000	1.275000
cd-o2	1039.400000	1.275000
cd-o3	1039.400000	1.275000
cd-o4	1039.400000	1.275000
cd-cd	839.599976	1.428000
cc-cd	1001.799988	1.373000
ca-cc	770.200012	1.456000
ca-ca	922.200012	1.398000
cc-ha	698.200012	1.084000

Table S3: Morse bond potential parameters for $Cu_3(HHTP)_2$ MOF.

$$V_{Morse}(r) = E_0[(1 - e^{-K_{ij}(r_{ij}-r_0)})^2 - 1] \qquad (3)$$

Bond type (Morse)	E_0(kcal mol^{-1})	r_0(Å)	K_{ij}(Å^{-1})
Cu-o1	377.652433	2.000318	0.796643
Cu-o2	345.598932	2.039822	0.408112
Cu-o3	276.258160	2.016915	1.158078
Cu-o4	545.175119	1.970611	0.517874

Table S4: Bending potential parameters for $Cu_3(HHTP)_2$ MOF.

$$V_{angle}(\theta) = \frac{1}{2}K_{ijk}(\theta_{ijk} - \theta_0)^2 \qquad (4)$$

Angle type (Harmonic)	$K_{ijk}(\text{kcal mol}^{-1}\text{deg}^{-2})$	$\theta(°)$
Cu-o1-cd	132.416365	105.103340
Cu-o2-cd	210.382777	107.723868
Cu-o3-cd	57.652500	110.267558
Cu-o4-cd	198.251713	105.036526
o1-Cu-o2	290.461154	165.213724
o1-Cu-o3	212.535810	94.999561
o1-Cu-o4	285.623947	86.636287
o2-Cu-o3	193.430370	85.440569
o2-Cu-o4	236.467396	101.611571
o3-Cu-o4	283.944477	163.001614
cd-cd-o1	139.000000	117.300003
cd-cd-o2	139.000000	117.300003
cd-cd-o3	139.000000	117.300003
cd-cd-o4	139.000000	117.300003
cd-cc-ha	97.000000	121.699997
cc-cd-o1	140.199997	120.300003
cc-cd-o2	140.199997	120.300003
cc-cd-o3	140.199997	120.300003
cc-cd-o4	140.199997	120.300003
cc-cd-cd	136.399994	114.099998
ca-cc-cd	135.199997	113.500000
ca-cc-ha	91.599998	124.000000
ca-ca-cc	130.000000	120.699997
ca-ca-ca	133.240000	120.020000

Table S5: Torsion potential parameters for $Cu_3(HHTP)_2$ MOF.

$$V_{torsion}(\phi) = K_{ijkl}[1 + \cos(m\phi_{ijkl} - \delta)] \qquad (5)$$

Dihedral type (Cosine)	K_{ijkl}(kcal mol^{-1})	$\delta(°)$	m
o1-Cu-o2-cd	5.559125	180.0000	2
o1-Cu-o3-cd	7.027488	180.0000	2
o1-Cu-o4-cd	6.090330	180.0000	2
o2-Cu-o1-cd	4.343647	180.0000	2
o2-Cu-o3-cd	2.000299	180.0000	2
o2-Cu-o4-cd	6.967154	180.0000	2
o3-Cu-o1-cd	2.495295	180.0000	2
o3-Cu-o2-cd	4.430417	180.0000	2
o3-Cu-o4-cd	2.641955	180.0000	2
o4-Cu-o1-cd	0.367073	180.0000	2
o4-Cu-o2-cd	2.147997	180.0000	2
o4-Cu-o3-cd	3.495792	180.0000	2
cc-cd-o2-Cu	1.972223	180.0000	2
cd-cd-o3-Cu	1.783663	180.0000	2
cd-cd-o4-Cu	1.928278	180.0000	2
cc-cd-o3-Cu	3.132602	180.0000	2
cc-cd-o4-Cu	0.127274	180.0000	2
cd-cd-o1-Cu	1.607713	180.0000	2
cd-cd-o2-Cu	1.385652	180.0000	2
cc-cd-o1-Cu	0.235726	180.0000	2
ca-cc-cd-o1	8.0000	180.0000	2
ca-cc-cd-o2	8.0000	180.0000	2
ca-cc-cd-o3	8.0000	180.0000	2
ca-cc-cd-o4	8.0000	180.0000	2
ca-cc-cd-cd	8.0000	180.0000	2
ca-ca-cc-ha	1.4000	180.0000	2
ca-ca-cc-cd	1.4000	180.0000	2
cc-cd-cd-o1	8.0000	180.0000	2
cc-cd-cd-o2	8.0000	180.0000	2
cc-cd-cd-o3	8.0000	180.0000	2
cc-cd-cd-o4	8.0000	180.0000	2
o1-cd-cd-o4	8.0000	180.0000	2
ha-cc-cd-o1	8.0000	180.0000	2
cc-ca-ca-cc	7.2500	180.0000	2
cc-ca-ca-ca	7.2500	180.0000	2
cc-cd-cd-cc	8.0000	180.0000	2
ha-cc-cd-o2	8.0000	180.0000	2
ha-cc-cd-cd	8.0000	180.0000	2
o2-cd-cd-o3	8.0000	180.0000	2
ha-cc-cd-o3	8.0000	180.0000	2
ha-cc-cd-o4	8.0000	180.0000	2
ca-ca-ca-ca	7.2500	180.0000	2
cc-cd-cd-o1	0.5500	180.0000	2
cc-cd-cd-o2	0.5500	180.0000	2
cc-cd-cd-o3	0.5500	180.0000	2
cc-cd-cd-o4	0.5500	180.0000	2
ca-cc-ca-ca	0.5500	180.0000	2
ca-cd-cc-ha	0.5500	180.0000	2

Table S6: Electrostatic and Lennard-Jones non-bonded parameters for $Cu_3(HTTP)_2$ MOF where r_{ij} refers to the distance between two atoms.

$$V_{LJ}(r) = 4\epsilon\left[\left(\frac{\sigma}{r_{ij}}\right)^{12} - \left(\frac{\sigma}{r_{ij}}\right)^{6}\right] \tag{6}$$

Atom name	Atom type	Charge	ε (kcal·mol^{-1})	σ / 2 (Å)
Cu	Cu	0.7484	0.00500	1.55700
s1	s1	−0.3175	0.25000	1.78180
s2	s2	−0.3091	0.25000	1.78180
s3	s3	−0.3077	0.25000	1.78180
s4	s4	−0.3198	0.25000	1.78180
cd	C	0.0711	0.08600	1.69983
cc	C	−0.0757	0.08600	1.69983
ca	C	−0.0318	0.08600	1.69983
ha	H	0.1628	0.01500	1.29982

Table S7: Harmonic bond potential parameters for $Cu_3(HTTP)_2$ MOF.

$$V_{bond}(r) = \frac{1}{2}K_{ij}(r_{ij} - r_0)^2 \qquad (7)$$

Bond type (Harmonic)	K_{ij}(kcal mol^{-1}Å^{-2})	r_0(Å)
cd-s1	463.399994	1.811000
cd-s2	463.399994	1.811000
cd-s3	463.399994	1.811000
cd-s4	463.399994	1.811000
cd-cd	839.599976	1.428000
cc-cd	1001.799988	1.373000
ca-cc	770.200012	1.456000
ca-ca	922.200012	1.398000
cc-ha	698.200012	1.084000

Table S8: Morse bond potential parameters for $Cu_3(HTTP)_2$ MOF.

$$V_{Morse}(r) = E_0[(1 - e^{-K_{ij}(r_{ij}-r_0)})^2 - 1] \qquad (8)$$

Bond type (Morse)	E_0(kcal mol^{-1})	r_0(Å)	K_{ij}(Å^{-1})
Cu-s1	176.105763	2.174445	1.226690
Cu-s2	243.312972	2.173174	0.859784
Cu-s3	269.721479	2.152024	0.126987
Cu-s4	101.289226	2.161108	1.436368

Table S9: Bending potential parameters for $Cu_3(HTTP)_2$ MOF.

$$V_{angle}(\theta) = \frac{1}{2} K_{ijk} (\theta_{ijk} - \theta_0)^2 \qquad (9)$$

Angle type (Harmonic)	K_{ijk}(kcal mol^{-1}deg^{-2})	$\theta(^\circ)$
Cu-s1-cd	168.511551	103.797253
Cu-s2-cd	283.297618	114.583964
Cu-s3-cd	180.965310	104.077062
Cu-s4-cd	75.003505	96.205808
s1-Cu-s2	124.914670	177.424257
s1-Cu-s3	184.081253	105.330430
s1-Cu-s4	239.120521	100.701571
s2-Cu-s3	135.957657	103.324626
s2-Cu-s4	284.248909	84.765014
s3-Cu-s4	75.475288	179.037112
cd-cd-s1	118.400002	128.199997
cd-cd-s2	118.400002	128.199997
cd-cd-s3	118.400002	128.199997
cd-cd-s4	118.400002	128.199997
cd-cc-ha	97.000000	121.699997
cc-cd-s1	121.199997	124.500000
cc-cd-s2	121.199997	124.500000
cc-cd-s3	121.199997	124.500000
cc-cd-s4	121.199997	124.500000
cc-cd-cd	136.399994	114.099998
ca-cc-cd	135.199997	113.500000
ca-cc-ha	91.599998	124.000000
ca-ca-cc	130.000000	120.699997
ca-ca-ca	133.240000	120.020000

Table S10: Torsion potential parameters for $Cu_3(HTTP)_2$ MOF.

$$V_{torsion}(\phi) = K_{ijkl}[1 + \cos(m\phi_{ijkl} - \delta)] \qquad (10)$$

Dihedral type (Cosine)	K_{ijkl}(kcal mol^{-1})	$\delta(°)$	m
s1-Cu-s2-cd	0.052620	180.0000	2
s1-Cu-s3-cd	4.397862	180.0000	2
s1-Cu-s4-cd	6.125540	180.0000	2
s2-Cu-s1-cd	0.065842	180.0000	2
s2-Cu-s3-cd	1.987909	180.0000	2
s2-Cu-s4-cd	3.989231	180.0000	2
s3-Cu-s1-cd	7.649231	180.0000	2
s3-Cu-s2-cd	6.141813	180.0000	2
s3-Cu-s4-cd	0.014565	180.0000	2
s4-Cu-s1-cd	0.986985	180.0000	2
s4-Cu-s2-cd	2.699931	180.0000	2
s4-Cu-s3-cd	0.031372	180.0000	2
cc-cd-s1-Cu	4.524151	180.0000	2
cc-cd-s2-Cu	6.212492	180.0000	2
cc-cd-s3-Cu	4.868993	180.0000	2
cc-cd-s4-Cu	5.888075	180.0000	2
cd-cd-s1-Cu	7.354385	180.0000	2
cd-cd-s2-Cu	3.529727	180.0000	2
cd-cd-s3-Cu	4.459797	180.0000	2
cd-cd-s4-Cu	7.954819	180.0000	2
ca-cc-cd-s1	12.0000	180.0000	2
ca-cc-cd-s2	12.0000	180.0000	2
ca-cc-cd-s3	12.0000	180.0000	2
ca-cc-cd-s4	12.0000	180.0000	2
ca-cc-cd-cd	12.0000	180.0000	2
ca-ca-cc-ha	5.6000	180.0000	2
ca-ca-cc-cd	5.6000	180.0000	2
cc-cd-cd-s1	12.0000	180.0000	2
s1-cd-cd-s4	12.0000	180.0000	2
ha-cc-cd-s1	12.0000	180.0000	2
cc-ca-ca-cc	9.0000	180.0000	2
cc-ca-ca-ca	7.2500	180.0000	2
cc-cd-cd-cc	12.0000	180.0000	2
cc-cd-cd-s3	12.0000	180.0000	2
ha-cc-cd-s2	12.0000	180.0000	2
ha-cc-cd-cd	12.0000	180.0000	2
cc-cd-cd-s2	12.0000	180.0000	2
s2-cd-cd-s3	12.0000	180.0000	2
ha-cc-cd-s3	12.0000	180.0000	2
ha-cc-cd-s4	12.0000	180.0000	2
cc-cd-cd-s4	12.0000	180.0000	2
ca-ca-ca-ca	7.2500	180.0000	2
cc-cd-cd-s1	0.5500	180.0000	2
cc-cd-cd-s2	0.5500	180.0000	2
cc-cd-cd-s3	0.5500	180.0000	2
cc-cd-cd-s4	0.5500	180.0000	2
ca-cc-ca-ca	0.5500	180.0000	2
ca-cd-cc-ha	0.5500	180.0000	2

S2. Validation of the developed force fields

The developed force fields are validated against available experimental data. The interlayer distances obtained from our MD simulations were compared to the experimentally measured powder X-ray diffraction data as shown in Figure S2. We have used Bragg's equation ($\lambda = 2d\sin(\theta)$) to calculate the interlayer distance in the dry MD equilibrated $Cu_3(HHTP)_2$ MOF with a broad peak at $2\theta = 24.9°$ resulting in a value of 0.357 nm. In comparison, the experimentally measured value for the interlayer distance corresponding to the broad peak at $2\theta = 28.17°$ is 0.316 nm (see Figure S2).
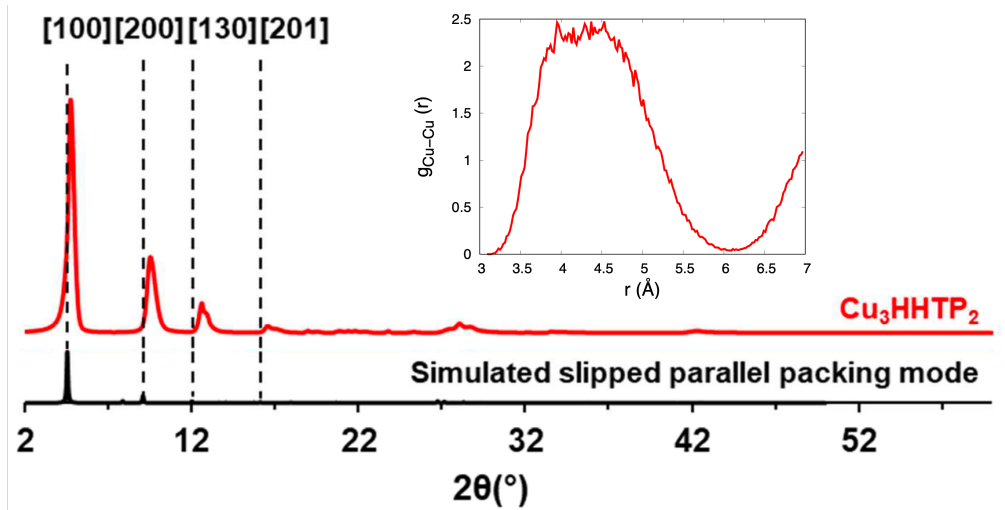
Figure S2: Experimental powder X-Ray diffraction pattern for $Cu_3(HHTP)_2$ 2D MOF adapted from the SI of Ref. 12. This pattern is in agreement with the previously reported PXRD data.[1] The radial distribution function (RDF) of Cu-Cu distance based on our MD simulations in the NPT ensemble at 293 K is also given.

The calculated radial distribution functions (RDFs) of Cu-Cu distances shows a prominent broad peak centered ~4.2 Å. Further validation of the developed force field comes from comparison of force field energies to the *ab initio* reference ones with respect to the change in Cu-O (Figure S3) and Cu-S (Figure S4) bond lengths.
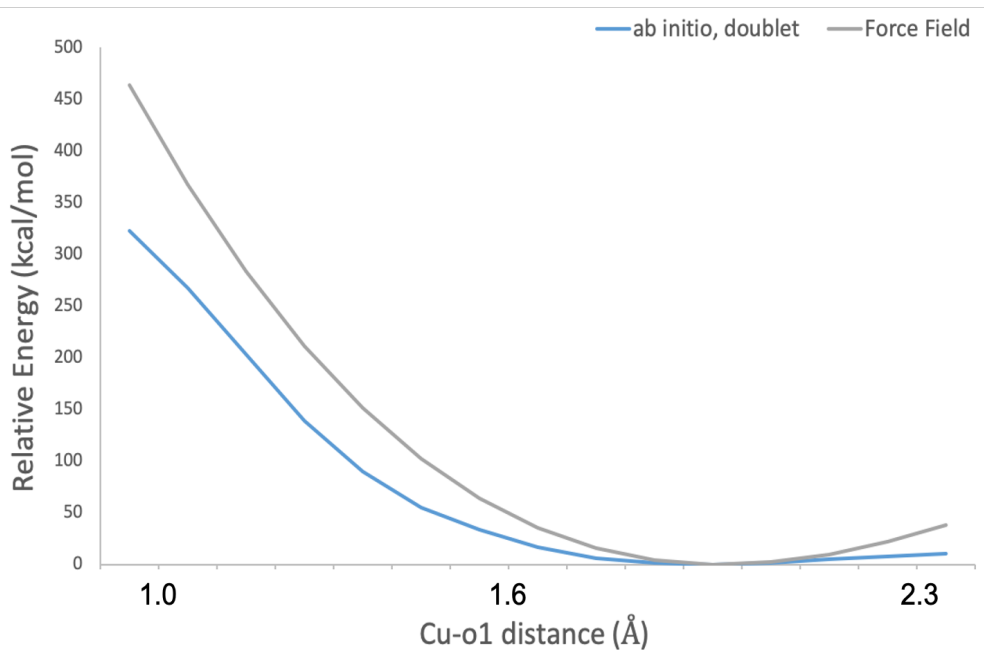
Figure S3: Comparison of our force field and reference *ab initio* energies at the ωB97M-v/def2-TZVP level for the doublet spin state of the copper catecholate cluster model shown in Figure S1. To obtain these correlation plots, the Cu-o1 bond is scanned from 0.95 Å to 2.35 Å.
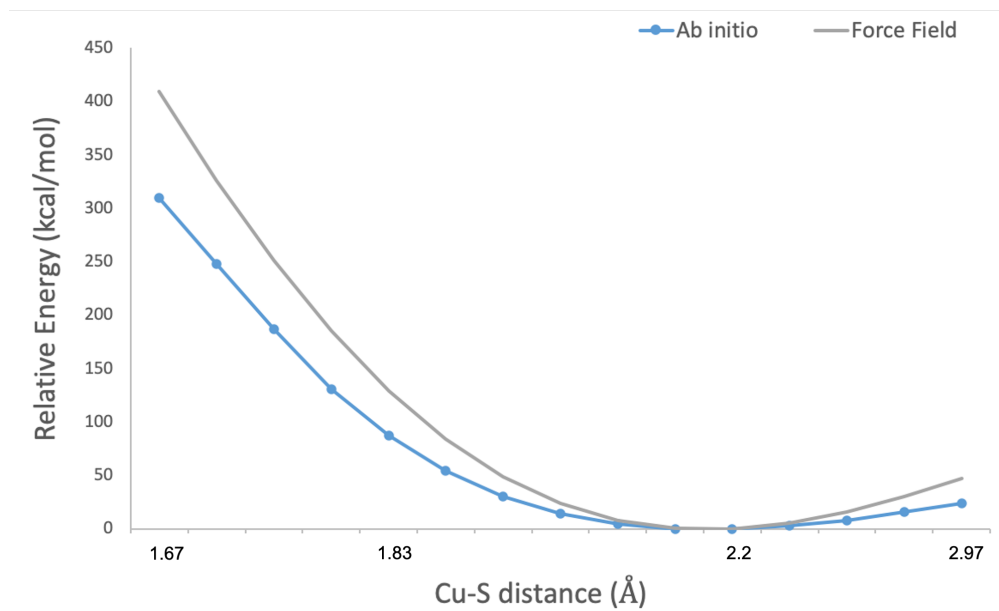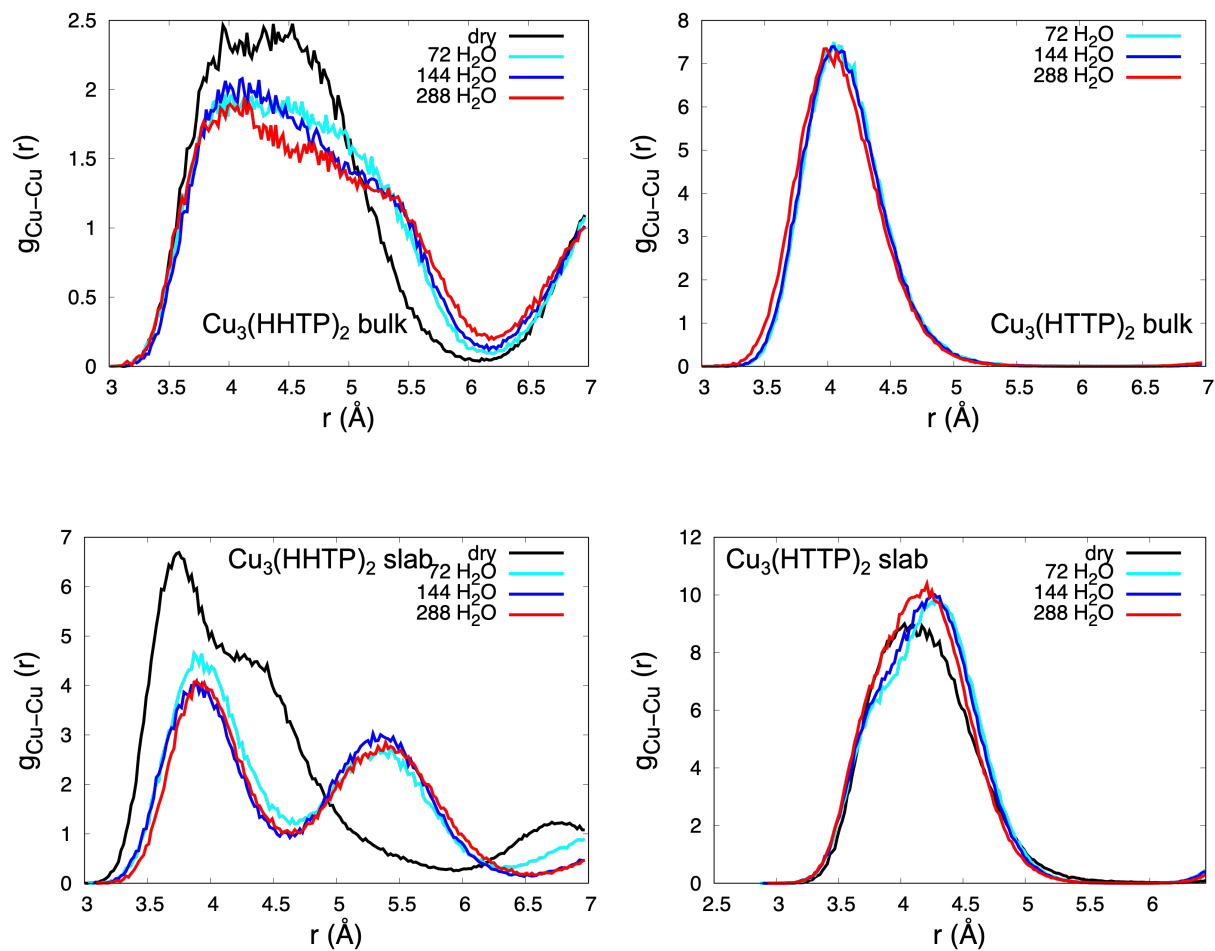
Figure S4: Comparison of our force field and reference *ab initio* energies at the ωB97M-v/def2-TZVP level for the doublet spin state of the copper thio-catecholate cluster model shown in Figure S1. To obtain these correlation plots, the Cu-s1 bond is scanned from 1.67 Å to 2.97 Å.

Figure S5: Calculated Cu-Cu RDFs of the bulk and slab models of all the studied dry and hydrated systems with different water loadings.

S4. Details of MD simulations

Classical MD simulations for dry MOFs were performed on the hexagonal ($\alpha = \beta = 90°$, $\gamma = 120°$, $a = b = 44.260$ Å, and $c = 23.007$ Å) hexa-layered 2×2×3 supercell of the bulk $Cu_3(HHTP)_2$ and $Cu_3(HTTP)_2$ MOFs (comprised of 1512 atoms in total and 72 metal centers) using DL_POLY Quantum v1.0 package.[14] Each dry system was equilibrated for 5 ns in the isothermal-isobaric NPT ensemble with a time step of 0.2 fs at 293 K temperature and 1 atm pressure, the experimental conditions at which the original $Co_3(HHTP)_2$ crystals were synthesized,[1] allowing the simulation box to vary. Analyzing changes in total energy of the systems over time confirms that 5 ns is indeed enough in order to reach an equilibrated stage. All systems were equilibrated in the isothermal-isobaric NPT ensemble with a time step of 0.2 fs. To study dynamics of confined water, we placed $n = 72$, 144, 216 and 288 water molecules inside the equilibrated dry MOF using PACKMOL[15] code. All simulations were carried out at 293 K temperature and 1 atm pressure. The equations of motion were propagated according to the velocity-Verlet algorithm. The temperature was kept constant using a Nosé-Hoover chain comprised of four thermostats.[16] An atom-atom cutoff distance of 10.0 Å was employed for electrostatics and 12–6 Lennard–Jones interactions. The long-range electrostatic interactions were calculated using the Ewald summation method.[17] Lorentz-Berthelot mixing rules were used to drive cross interactions terms between water and the frameworks using the TIP4P/2005[18] water model. To model water molecules, we use the flexible 4-site q-TIP4P/F[19] water potential. The q-TIP4P/F water model has been shown to be successful in reproducing a diverse number of static and dynamical properties of water including melting point, diffusion coefficients and infrared spectrum. Dynamical properties were calculated from the average of 10 independent 50 ps NVE simulations. These trajectories were run from 10 different initial configurations obtained from a 10 ps NVT trajectory that followed the NPT simulations. The final snapshots of these NVT trajectories were then used as initial configurations for 50 ps NVE simulations ensuring that different starting configurations initiate independent NVE trajectories.
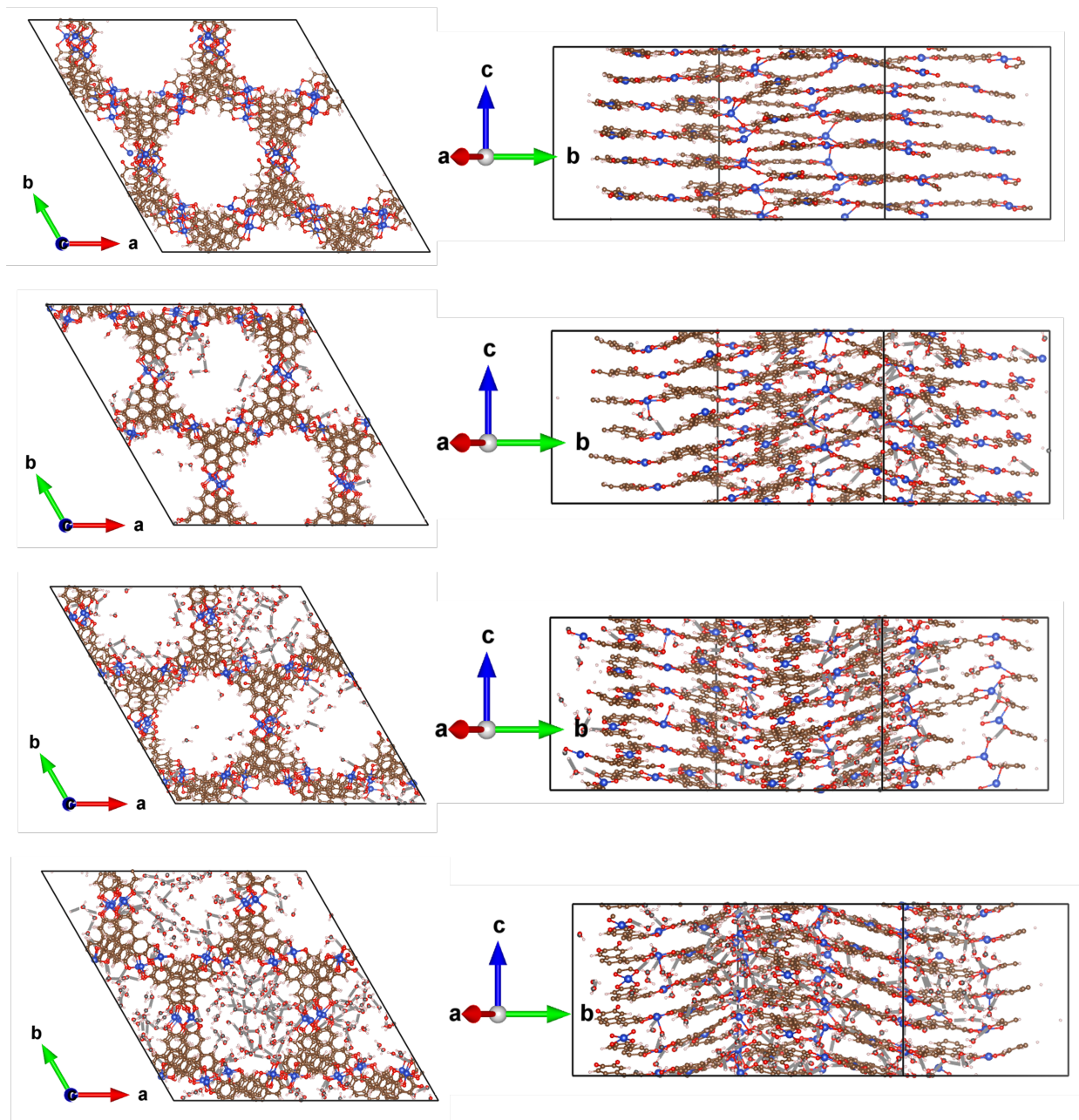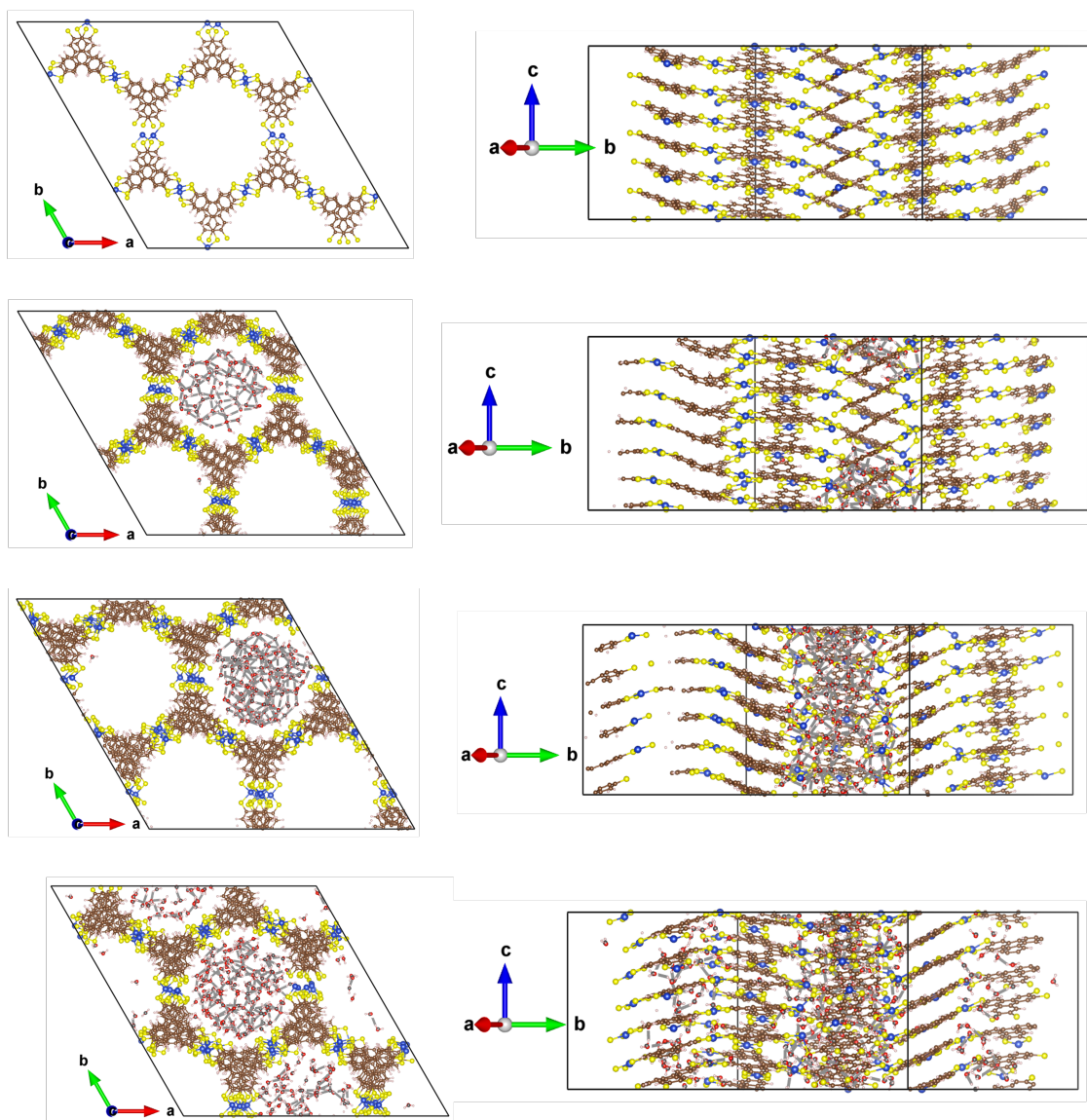
Figure S6: Top and side views of the 293 K MD equilibrated bulk models of $Cu_3(HHTP)_2$ dry and hydrated systems with $1H_2O/Cu^{2+}$ (72 H_2O, top), $2H_2O/Cu^{2+}$ (144 H_2O, middle) and $4H_2O/Cu^{2+}$ (288 H_2O, bottom) water molecules.

Figure S7: Top and side views of the 293 K MD equilibrated bulk models of $Cu_3(HTTP)_2$ dry and hydrated systems with $1H_2O/Cu^{2+}$ (72 H_2O, top), $2H_2O/Cu^{2+}$ (144 H_2O, middle) and $4H_2O/Cu^{2+}$ (288 H_2O, bottom) water molecules.
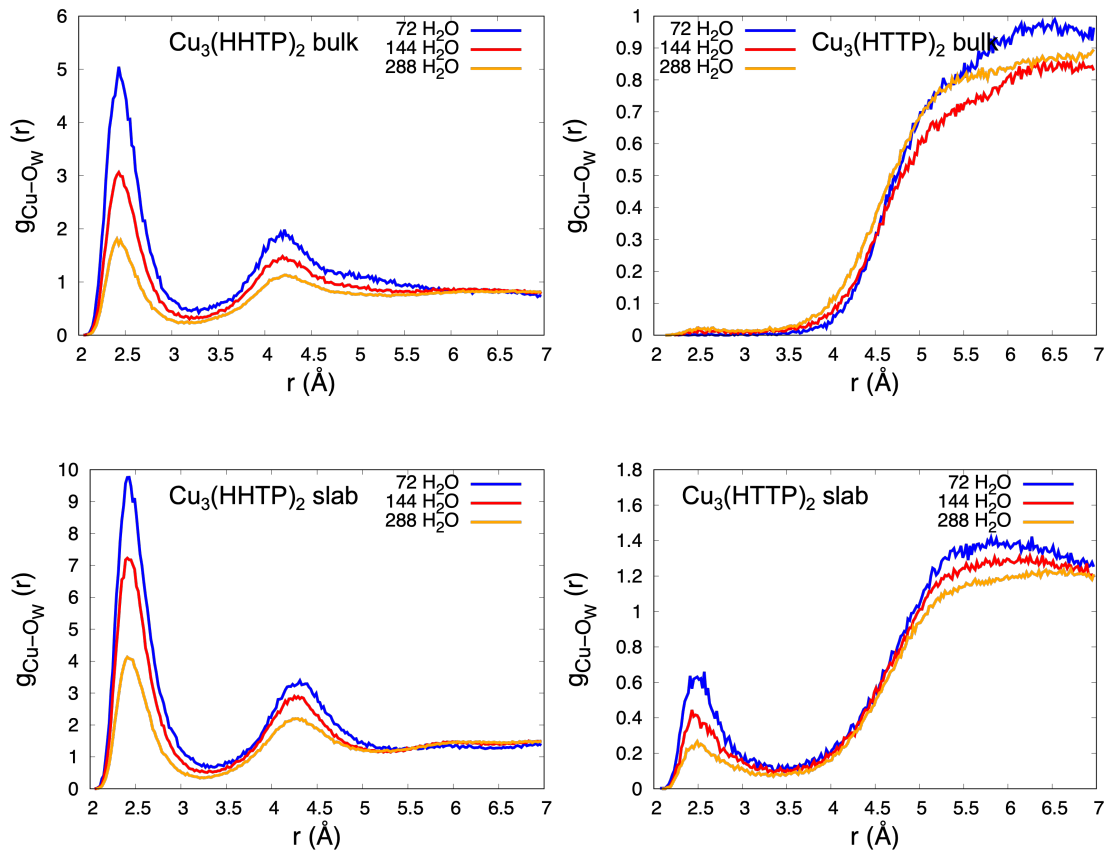
Figure S8: Calculated Cu-O$_W$ (oxygen of water) RDFs of the bulk and slab models of all studied hydrated systems with different water loadings.
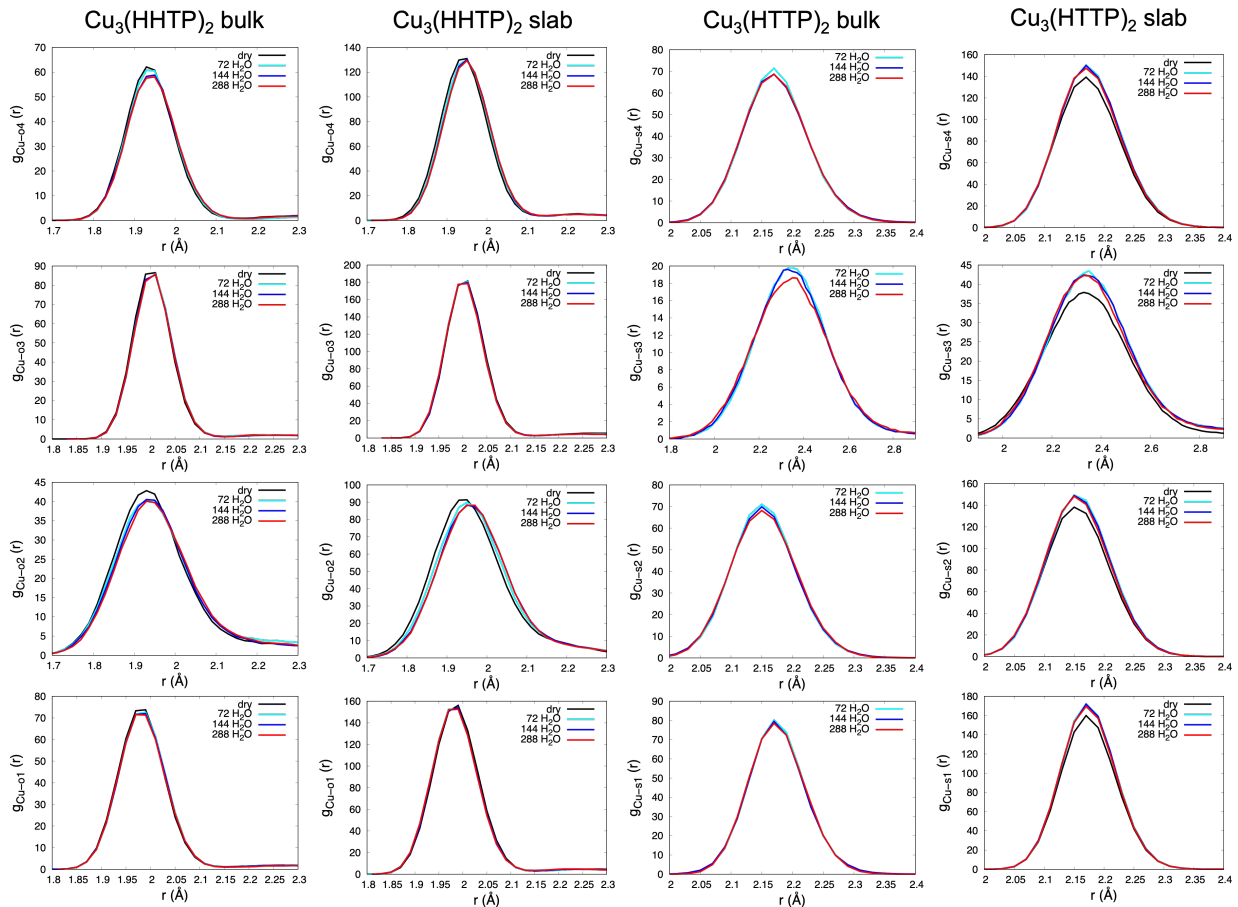
Figure S9: Calculated Cu-X$_n$ (X= O and S and n = 1–4) RDFs of the bulk and slab models of all studied dry and hydrated systems with different water loadings.
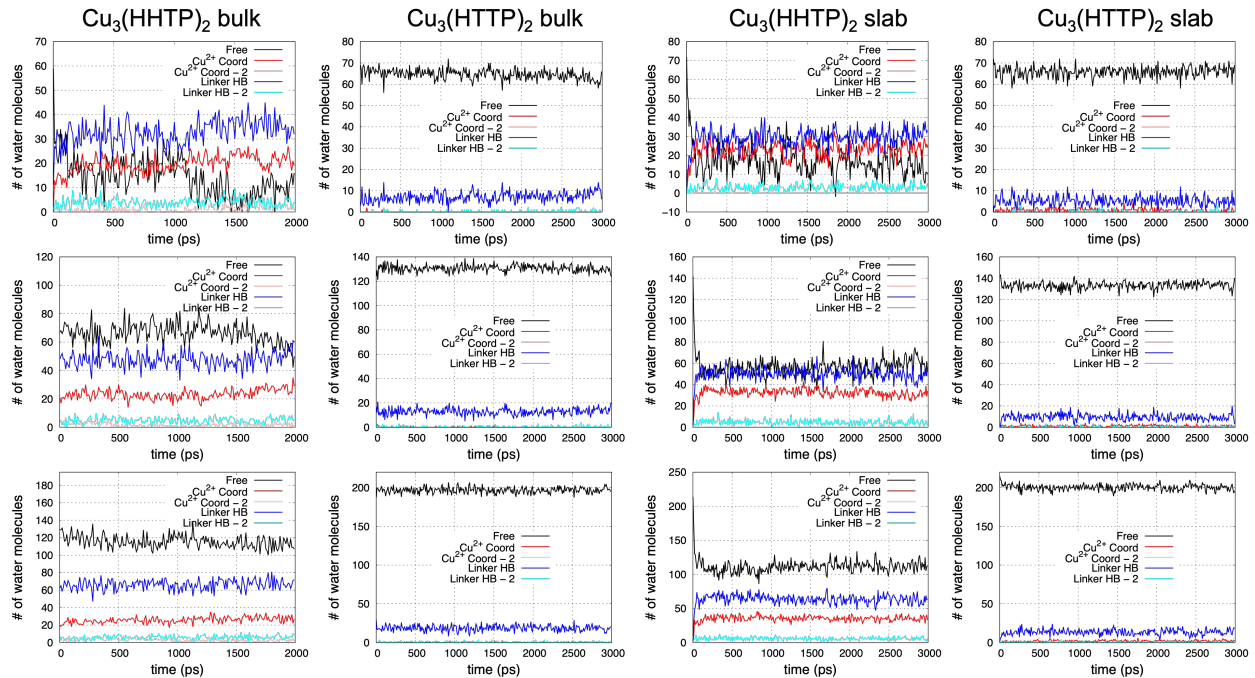
Figure S10: Calculated absolute changes in the number of different types of water molecules in the slab and bulk models of $Cu_3(HHTP)_2$ and $Cu_3(HTTP)_2$ MOFs with 1 H_2O (top row), 2 H_2O (middle row) and 3 H_2O (bottom row) molecules per Cu^{2+} metal centers.
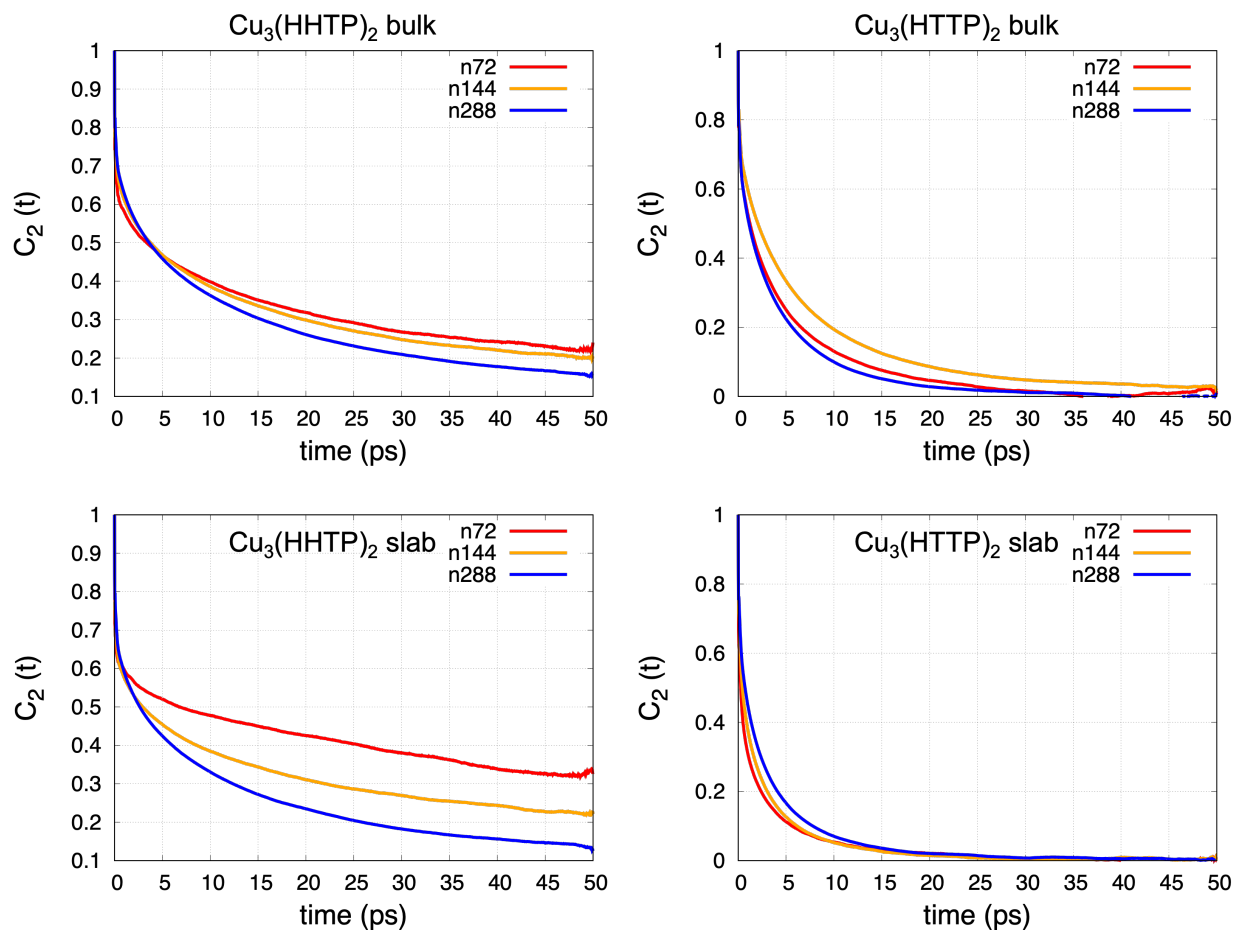
Figure S11: Orientational time correlation functions of the bulk and slab models of the $Cu_3(HHTP)_2$ and $Cu_3(HTTP)_2$ 2D MOFs with different water loadings.
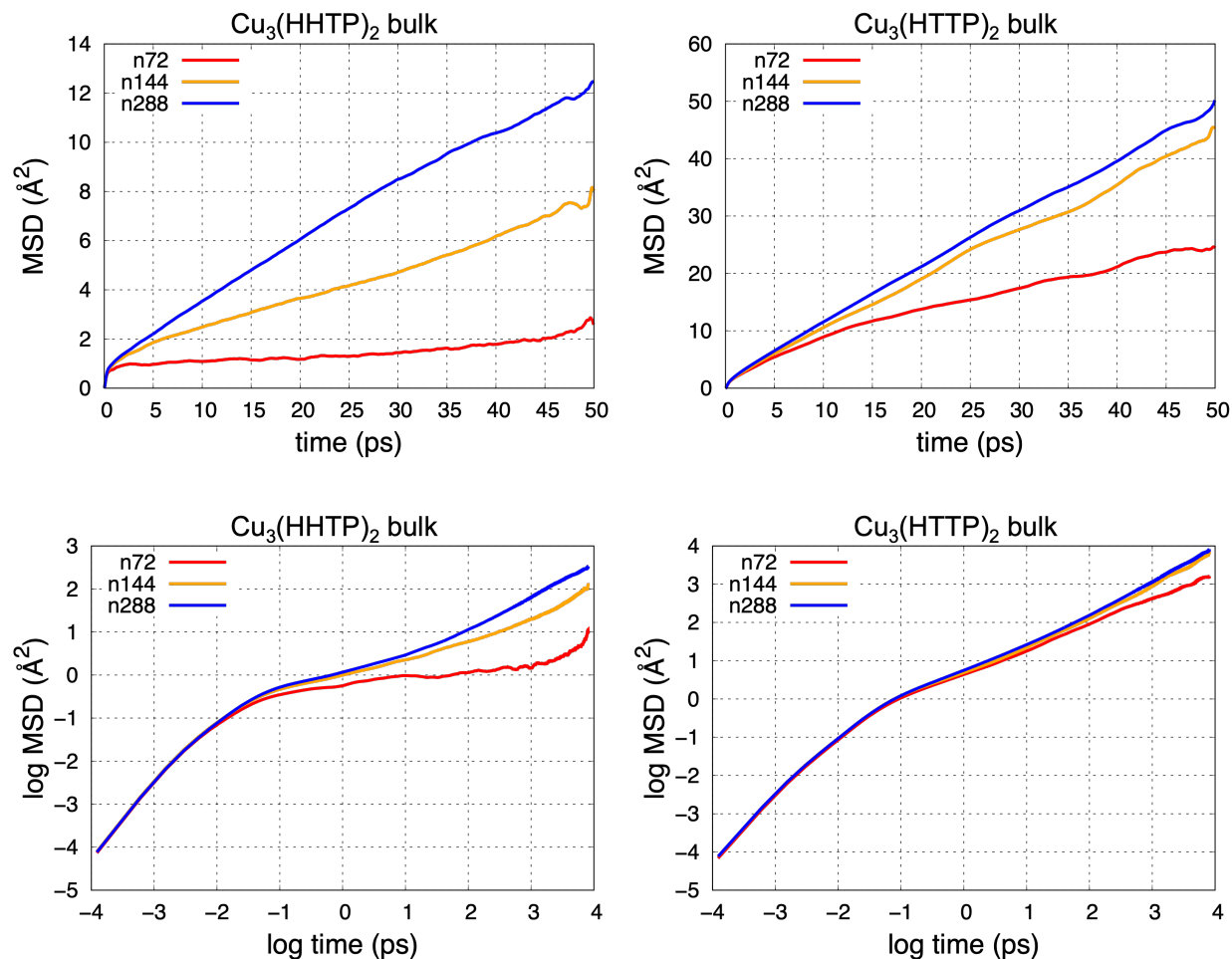
Figure S12: Mean Square Displacement (MSD) plots for bulk models of the $Cu_3(HHTP)_2$ and $Cu_3(HTTP)_2$ 2D MOFs with different water loadings obtained from 50 ps NVE simulations. The corresponding log-log plots are also shown.

Figure S13: Mean Square Displacement (MSD) plots for slab models of the $Cu_3(HHTP)_2$ and $Cu_3(HTTP)_2$ 2D MOFs with different water loadings obtained from 50 ps NVE simulations. The corresponding log-log plots are also shown.
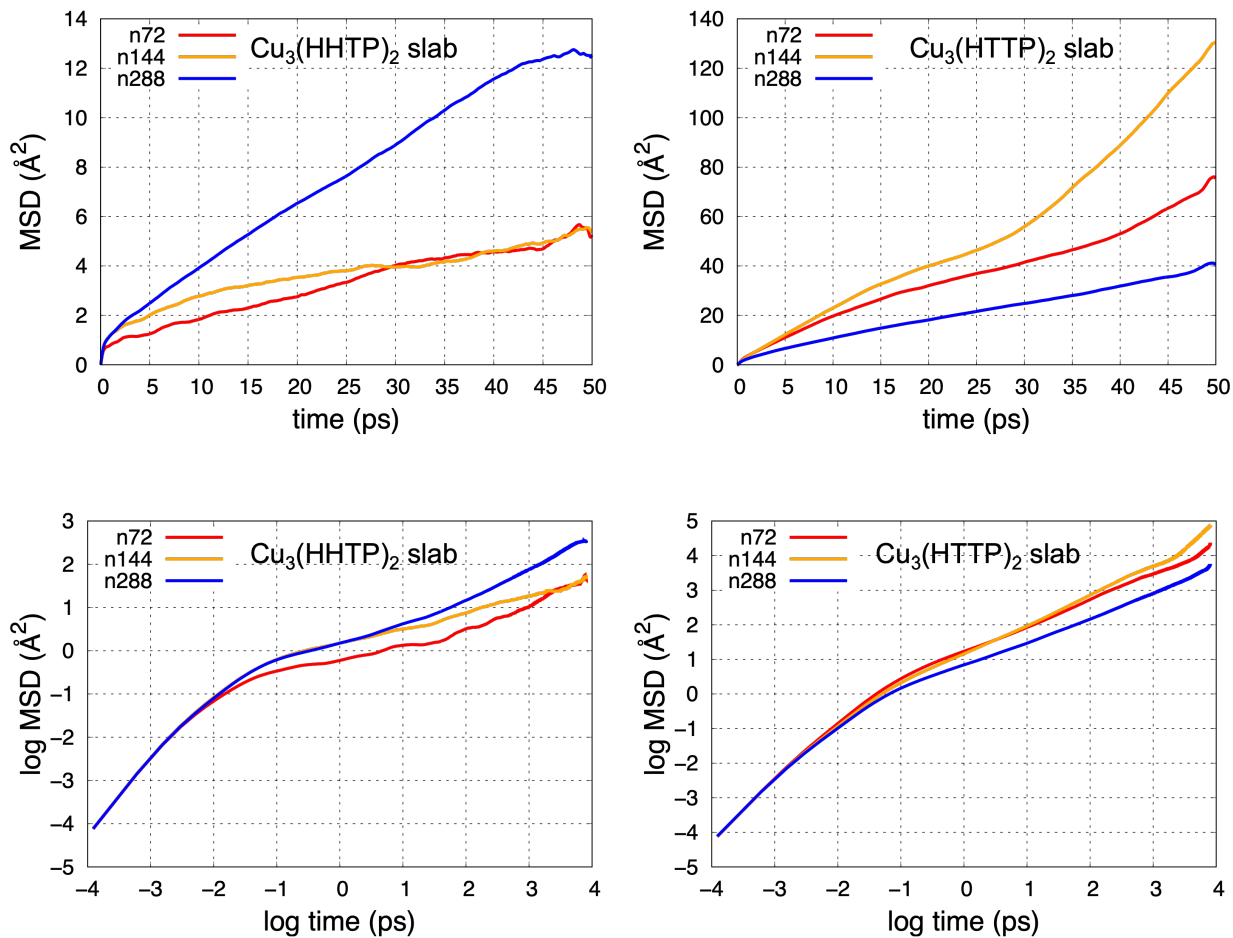
References

(1) Hmadeh, M. et al. New porous crystals of extended metal-catecholates. *Chem. Mater.* **2012**, *24*, 3511–3513.

(2) Perdew, J. P.; Burke, K.; Ernzerhof, M. Generalized Gradient Approximation Made Simple. *Phys. Rev. Lett.* **1996**, *77*, 3865–3868.

(3) Grimme, S.; Antony, J.; Ehrlich, S.; Krieg, H. A consistent and accurate ab initio parametrization of density functional dispersion correction (DFT-D) for the 94 elements H-Pu. *J. Chem. Phys.* **2010**, *132*, 154104.

(4) Hutter, J.; Iannuzzi, M.; Schiffmann, F.; VandeVondele, J. cp2k: atomistic simulations of condensed matter systems. *WIREs Computational Molecular Science* **2014**, *4*, 15–25.

(5) Goedecker, S.; Teter, M.; Hutter, J. Separable dual-space Gaussian pseudopotentials. *Phys. Rev. B* **1996**, *54*, 1703–1710.

(6) Wang, J.; Wolf, R. M.; Caldwell, J. W.; Kollman, P. A.; Case, D. A. Development and testing of a general amber force field. *J. Computat. Chem.* **2004**, *25*, 1157–1174.

(7) Goldberg, D. *Genetic Algorithms in Search, Optimization and Machine Learning,*; Addison-Wesley, 1989.

(8) Mardirossian, N.; Head-Gordon, M. ωB97M-V: A combinatorially optimized, range-separated hybrid, meta-GGA density functional with VV10 nonlocal correlation. *J. Chem. Phys.* **2016**, *144*, 214110.

(9) Shao, Y.; Gan, Z.; Epifanovsky, E.; Gilbert, A. T.; Wormit, M.; Kussmann, J.; Lange, A. W.; Behn, A.; Deng, J.; Feng, X., et al. Advances in molecular quantum chemistry contained in the Q-Chem 4 program package. *Mol. Phys.* **2015**, *113*, 184–215.

(10) Breneman, C. M.; Wiberg, K. B. Determining atom-centered monopoles from molecular electrostatic potentials. The need for high sampling density in formamide conformational analysis. *J. Comput. Chem.* **1990**, *11*, 361–373.

(11) Rappe, A. K.; Casewit, C. J.; Colwell, K. S.; III, W. A. G.; Skiff, W. M. UFF, a full periodic table force field for molecular mechanics and molecular dynamics simulations. *J. Am. Chem. Soc.* **1992**, *114*, 10024–10035.

(12) Mendecki, L.; Mirica, K. Conductive metal–organic frameworks as ion-to-electron transducers in potentiometric sensors. *ACS Appl. Mater. Interfaces* **2018**, *10*, 19248–19257.

(13) Day, R. W.; Bediako, D. K.; Rezaee, M.; Parent, L. R.; Skorupakii, G.; Arguilla, M. Q.; Hendon, C. H.; Stassen, I.; Gianneschi, N. C.; Kim, P.; Dincă, M. Single Crystals of Electrically Conductive Two-Dimensional Metal-Organic Frameworks: Structural and Electrical Transport Properties. *ACS Cent. Sci.* **2019**, *5*, 1959–1964.

(14) Momeni, M. R.; Shakib, F. A. The DL_POLY Quantum molecular simulation package. Available from: https://github.com/fashakib/DL_POLY-Quantum-v1.0.

(15) Martínez, L.; Andrade, R.; Birgin, E. G.; Martínez, J. M. PACKMOL: A package for building initial configurations for molecular dynamics simulations. *J. Comput. Chem.* **2009**, *30*, 2157–2164.

(16) Tuckerman, M. E. *Statistical mechanics: Theory and molecular simulation*; (Oxford University Press, 2010.

(17) Leach, A. R. *Molecular modeling: Principles and applications*; Pearson Prentice Hall, 2001.

(18) Abascal, C., J. L. F.; Vega A general purpose model for the condensed phases of water: TIP4P/2005. *J. Chem. Phys.* **2005**, *123*, 234505.

(19) Habershon, T. E. M. D. E., S.; Markland Competing quantum effects in the dynamics of a flexible water model. *J. Chem. Phys.* **2009**, *131*, 024501.